CHEMISTRY OF MATERIALS
Communication
Cite This: Chem. Mater. 2017, 29, 8963-8967
pubs.acs.org/cm

Revisiting the Incorporation of Ti(IV) in UiO-type Metal–Organic Frameworks: Metal Exchange versus Grafting and Their Implications on Photocatalysis

Jara G. Santaclara,[†] Alma I. Olivos-Suarez,[*,†] Adrian Gonzalez-Nelson,[†] Dmitrii Osadchii,[†,‡] Maxim A. Nasalevich,[†] Monique A. van der Veen,[†] Freek Kapteijn,[†] Alena M. Sheveleva,[§] Sergey L. Veber,[§] Matvey V. Fedin,[§] Alexander T. Murray,[*,⊥] Christopher H. Hendon,[*,∥] Aron Walsh,[¶,□] and Jorge Gascon[*,†,‡]

[†]Catalysis Engineering, Department of Chemical Engineering, Delft University of Technology, van der Maasweg 9 2629 HZ, Delft, The Netherlands

[‡]King Abdullah University of Science and Technology, KAUST Catalysis Center, Advanced Catalytic Materials, Thuwal 23955, Saudi Arabia

[§]International Tomography Center, Novosibirsk State University, Novosibirsk 630090, Russia

[⊥]Department of Chemistry, Massachusetts Institute of Technology, Cambridge, Massachusetts 02139, United States

[∥]Department of Chemistry and Biochemistry, University of Oregon, Eugene, Oregon 97403, United States

[¶]Department of Materials, Imperial College London, London SW7 2AZ, U.K.

[□]Global E3 Institute and Department of Materials Science and Engineering, Yonsei University, Seoul 120-749, South Korea

Supporting Information

Generation of hydrogen from water (hydrogen evolution reaction, HER) mediated by sunlight is a key challenge in the design of new energy conversion paradigms.[1] While there are many classes of materials that will promote this reaction, metal–organic frameworks (MOFs) have emerged as promising platforms owing to their high surface area, structural diversity, and late-stage tunability.[2] However, most MOFs suffer from hydrolytic instability, limiting their application in aqueous HER photocatalytic systems.[3,4] MOFs of the UiO series possess good water and thermal stability and opportunities for postsynthetic modification.[5,6]

Common strategies for functionalization of Zr-UiO-type materials include linker modification and metal incorporation.[7−9] The former has been extensively studied in both UiO- and MIL-125-type materials through utilization of functionalized ligands.[10−12] For example, amination of the terephthalic acid linker in MIL-125 has been shown to close the band gap, redshifting from the UV and thus enabling visible light photocatalysis. In the case of UiO-66, the addition of Ti(IV) has been extensively studied because of its photoaccessible unoccupied Ti(III) state, but nevertheless, the structural characterization of these materials remains largely unknown.[13−18]

The two hypotheses for how incorporation of Ti into UiO-66 occurs are either through metal exchange into the inorganic secondary building unit (SBU) or grafting of the Ti(IV) onto the surface of this node at a linker vacancy site (Figure 1). Metal exchange has been attempted primarily with $TiCl_4$·2THF as a Ti(IV) source, but the nature of this exchange is inconclusive.[8,14,19−21]

A major impediment to the understanding of metal inclusion in UiO-type materials, either as ion exchange or metal appendage, is that while Ti(IV) can also be conjectured to occupy linker vacancy sites, until recently, the nature of these vacancies was poorly understood.[22,23] However, recent advances in the characterization of UiO defect chemistry has revealed up to 33% linker vacancies,[24−30] and the nature of these vacancies has been systematically explored in the related NU-1000 MOF and the MOF-801 series.[31,32]

An ideal Ti(III) photocatalyst features low energy unoccupied Ti(IV) orbitals that allow facile electron occupation of this state

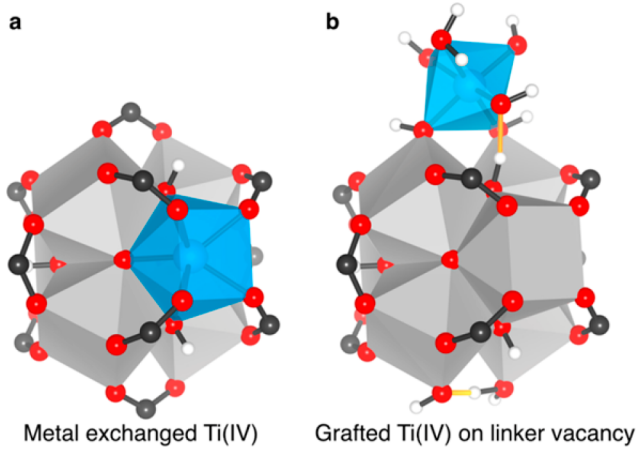

Figure 1. Proposed coordination sites of Ti in UiO-type materials. (a) Inclusion of Ti(IV) in the cluster through metal exchange. (b) Appendage of Ti(IV) to the surface of the cluster at a linker vacancy defect site.

Received: August 8, 2017
Revised: October 17, 2017
Published: October 17, 2017

DOI: 10.1021/acs.chemmater.7b03320
Chem. Mater. 2017, 29, 8963−8967

upon photoirradiation and a local electron rich ligand that can transiently stabilize a proton (e.g., a bridging oxo as found in MIL-125 or pendant hydroxy/alkoxy motif).[33,34] Hence, density functional theory (DFT) calculations are able to systematically elucidate the nature of the frontier bands for different Ti coordination environments in UiO-66. The UiO-66 material's frontier orbitals are defined by a ligand−ligand transition (Figure 2).[35] Amination of the linker (i.e., NH_2-UiO-66(Zr), **1**) yields an occupied midgap state, albeit still with a ligand-based transition (Figure 2).[36] We then investigated the energies of Ti both in the cluster (metal exchange) and on a defect site (metal appendage) in both the aminated and native frameworks. When Ti is incorporated in the cluster, the valence bands are unaltered, and the conduction bands do not feature Ti orbitals at the frontier; rather, Ti orbitals are found at marginally higher energies but nevertheless should be photoaccessible. Likewise, with Ti appended on defect sites, the conduction band is not defined primarily by Ti orbitals.

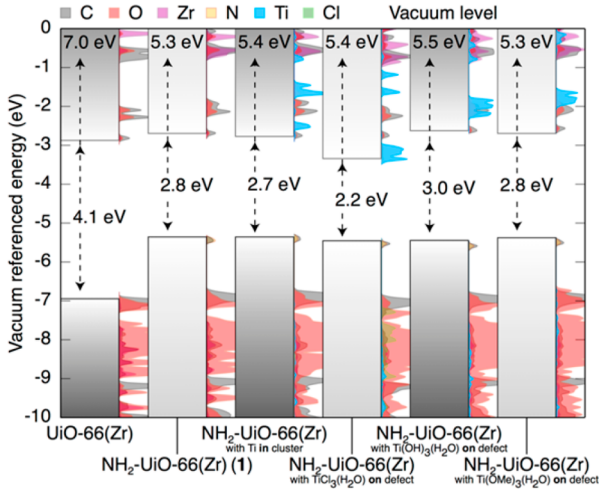

Figure 2. Density of states (DOS) and band alignment of native Zr-UiO-66, the 16%-NH_2-UiO-66(Zr) (**1**), compared to the models with Ti(IV) inside the SBU or appended to the linker defect site and passivated with Cl^-, ^-OH, or ^-OMe. A single H_2O is included to complete the octahedral coordination sphere. DOS at ∼5.4 and ∼2.9 eV have amino-benzene parentage.

These calculations assume that additional ligands on titanium are hydroxyl groups. With a weaker-field ligand such as Cl^-, the Ti(IV) unoccupied state is stabilized, thus bringing Ti orbitals to the frontier, Figure 2. Therefore, the ligand set as well as the titanium site occupancy should be paramount in generating an active photocatalyst.

As our goal was to generate a visible-light active photocatalyst, we used the aminated precursor **1**. Initially, we attempted to functionalize **1** with $TiCl_4$·2THF using a method previously reported.[8] However, the material formed under these conditions, **1′**, simply featured an increase in linked vacancies as observed by an increase in the BET adsorption isotherm (Figures S1 and S2) and increasing infrared O−H stretching anisotropy (Figures S3 and S4). Additionally, we see both Ti and Cl inclusion by TEM/EDX (transmission electron microscopy/energy dispersive X-ray analysis, Figure S5). Given the propensity of Ti−Cl bonds to hydrolyze under the synthetic conditions (three days in methanol), we instead suspect Cl-termination of zirconium clusters and formation of $Ti(OR)_x$-type materials in the pore. Upon photoexcitation of **1′**, *X*/*Q*-band EPR (9/34 GHz) indicates electron transfer with a formation of Ti(III) in octahedral coordination environment, similar to that of MIL-125-NH_2 (Figure 5). However, the observation of sharp peaks with well resolved *g*-tensor components g = [1.976 1.945 1.925] is more consistent with a single Ti environment (e.g., $Ti(OR)_x$) rather than with the superposition of environments anticipated if Ti would reside at the defect sites (vide infra).

The photocatalytic hydrogen evolution activity of **1′** was found to be 1.5× greater than that of native **1** (Figure 3).

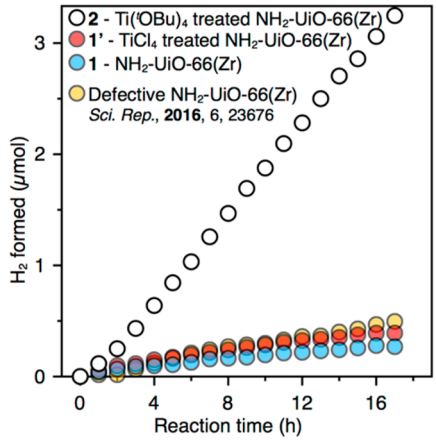

Figure 3. Photocatalytic activity of native NH_2-UiO-66(Zr) (**1**, blue) and a deliberately defective analogue (yellow) compared to that of the $TiCl_4$-loaded NH_2-UiO-66(Zr) (**1′**, red), and Ti(^{t}OBu)$_4$-treated NH_2-UiO-66(Zr) (**2**, white). Deliberately defective NH_2-UiO-66 was synthesized using the method presented in ref 35.

Indeed, this HER activity is in line with previously reported results for the defect-laden version of this material (data of the deliberately defective NH_2-UiO-66(Zr) showed a 1.7× increase in photocatalytic activity with approximately 30% linker vacancies).[36] From this data, we propose that Ti is not primarily responsible for catalytic activity in this case. Therefore, we developed a new synthetic route to minimize new linker vacancies formed during the metal inclusion.

The most frequently proposed defect passivation of the zirconia SBUs is through termination with pendant −OH groups that share a third proton in a bridging H-bond (depicted at the bottom of Figure 1b). We propose that use of a more basic Ti salt could deprotonate the defect site and thus enhance grafting of Ti onto the inorganic SBU. Thus, we selected Ti(^{n}OBu)$_4$ as the Ti(IV) source for postsynthetic modification of **1** to form a postulated Ti-grafted product referred to as **2** (depicted in Figure 1b). Given the reaction conditions, a representative model of the Ti-coordination sphere is likely either octahedral Ti(IV) with either associated hydroxides or alkoxides. The electronic structure of both systems is presented in Figure 2. **2** demonstrates the expected decrease in BET area, associated with the grafting of the Ti(IV) to the surface of the SBU, a single IR O−H stretching resonance, and a higher proportion of remaining residues of metal oxides observed by TGA (Figure S1, S3, and S6), corresponding to the appendage of a metal with no concurrent increase in site vacancies. Importantly, if metal exchange were occurring into the SBU, we would expect no decrease in the surface area.

TEM/EDS mapping of Ti shows good dispersion of Ti(IV) (Figure 4), with some preference for surface functionalization. EPR of the photoexcited material (X- and Q-band) in this case

DOI: 10.1021/acs.chemmater.7b03320
Chem. Mater. 2017, 29, 8963−8967

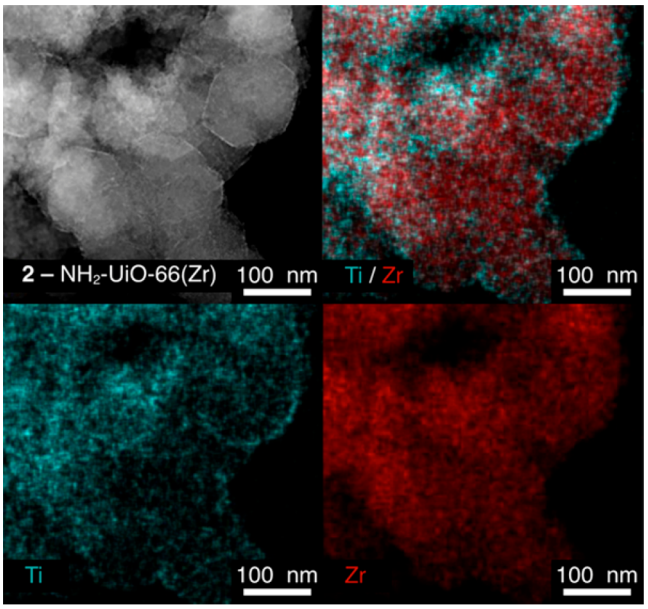

Figure 4. Transmission electron microscopy/energy dispersive X-ray spectroscopy images of NH_2-UiO-66(Zr) (**2**). Ti(IV) is present throughout the crystal with highest concentrations found on the crystal edges.

shows a more diffuse Ti^{III} signal relative to that of **1′** (Figure 5), indicative of a broader distribution of *g*-tensor components and

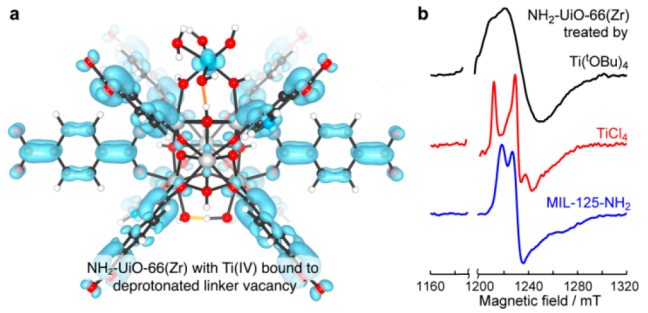

Figure 5. (a) Spin density of the pseudoexcited state of 16%-NH_2-UiO-66(Zr)-$Ti(OH)_3(H_2O)$ **2** shows a majority of spin contribution on the organic linker but, importantly, a minor contribution from a Ti(III) d-orbital. The Ti(III) density should increase proportionally with loading on the framework. (b) Q-band continuous wave EPR spectra (≈33.5 GHz) of photoexcited MIL-125-NH_2 **1′** and **2** in the reaction mixture of $CH_3CN/Et_3N/H_2O$.

suggesting a number of possible combinations of Ti-containing linker defects on Zr SBUs. Noteworthy, measurements of the T1 and T2 relaxation times of **2** are in good agreement for highly dispersed Ti(IV) through the UiO-66 lattice (Figure S11) and suggest that Ti is atomically dispersed. Long-range crystallinity appeared to be maintained, as observed by powder X-ray diffraction (PXRD) (Figure S7).

Most importantly, the grafted material **2** demonstrates significantly improved photocatalysis compared to the other materials considered here. Upon irradiation in $CH_3CN/Et_3N/H_2O$, hydrogen was evolved from water with a rate of 0.2 μmol h^{-1}, attributed to photocatalysis occurring at the Ti(III) sites (Figure 3). This corresponds to a rate 14× greater than either native NH_2-UiO-66(Zr) (**1**) or the material formed by Ti incorporation through treatment of **1** with $TiCl_4$·2THF (**1′**). Indeed, upon photoirradiation of **2** at 370 nm, a new transient absorption band centered at around 750 nm was observed (Figure S9) which, in agreement with EPR, likely corresponds to a Ti(III) excitation.[37−40]

From direct comparison of the **2**-Ti-Cl, −Ti-OH and −Ti-OMe structures, we see that the electron density of the ligand determines the extent of Ti contribution to the conduction band. While −Cl termination is electronically the most favorable, it is unlikely that such ligand environments persist under relevant reaction conditions. Despite both −OH and −OMe terminated models suggesting minimal Ti *d* orbital contributions to their conduction band minima, the ground state DFT calculation is not the most informative representation of the orbital density upon photoexcitation. Thus, we constructed a model of triple −OH terminated **2** and indeed find that most of the band is defined by the ligands, but there is additional highly localized titanium *d* character as a minor component (emphasized in Figure 5a). Two conclusions can be drawn from this calculation: (i) the titanium density of states will increase proportionally with the increased loading of Ti in the MOF and (ii) titanium density will increase proportionally to linker vacancies (either by increased loading of Ti-sites or by decreased linker contribution to the frontier bands).

In conclusion, we found that upon titanium incorporation into the MOF UiO-66, the type of Ti binding is through appendage of Ti to a linker vacancy rather than replacement of zirconium in the SBU. Careful choice of titanium source in the postsynthetic modification of this MOF determines the extent of covalent interaction between the MOF and Ti. Furthermore, the appendage of Ti(IV) to the surface of the MOF yields a moderately active HER photocatalyst. More active catalysts will likely spawn from the engineering the Ti-bound ligand set to achieve persistence in reaction conditions while being weakly electron donating (to lower the Ti(III) band deeper into the electronic band gap). Therefore, we showed that in MOF catalyst design, both the defect environment and external ligand field are equally important in the further improvement of activity in photocatalysis for this class of materials.

■ ASSOCIATED CONTENT

Supporting Information

The Supporting Information is available free of charge on the ACS Publications website at DOI: 10.1021/acs.chemmater.7b03320.

Comprehensive experimental details of PXRD, EPR, TEM/EDX, gas sorption isotherms, DRIFTS, diffuse reflectance UV−vis, DTAS, and computational methods (PDF)

■ AUTHOR INFORMATION

Corresponding Authors

*E-mail: a.i.olivossuarez@tudelft.nl.
*E-mail: chendon@uoregon.edu.
*E-mail: murraya@mit.edu.
*E-mail: jorge.gascon@kaust.edu.sa.

ORCID

Monique A. van der Veen: 0000-0002-0316-4639
Freek Kapteijn: 0000-0003-0575-7953
Sergey L. Veber: 0000-0002-5445-3713
Matvey V. Fedin: 0000-0002-0537-5755
Alexander T. Murray: 0000-0002-7914-8205

DOI: 10.1021/acs.chemmater.7b03320
Chem. Mater. 2017, 29, 8963−8967

Christopher H. Hendon: 0000-0002-7132-768X
Aron Walsh: 0000-0001-5460-7033
Jorge Gascon: 0000-0001-7558-7123

Notes

The authors declare no competing financial interest.

■ ACKNOWLEDGMENTS

This work used the Extreme Science and Engineering Discovery Environment (XSEDE), which is supported by National Science Foundation Grant ACI-1053575. S.L.V. and M.V.F. thank the Russian Science Foundation (Grant 14-13-00826).

■ REFERENCES

(1) Tachibana, Y.; Vayssieres, L.; Durrant, J. R. Artificial photosynthesis for solar water-splitting. *Nat. Photonics* **2012**, *6*, 511−518.
(2) Zhang, T.; Lin, W. Metal-organic frameworks for artificial photosynthesis and photocatalysis. *Chem. Soc. Rev.* **2014**, *43*, 5982−5993.
(3) Nasalevich, M. A.; van der Veen, M.; Kapteijn, F.; Gascon, J. Metal-organic frameworks as heterogeneous photocatalysts: advantages and challenges. *CrystEngComm* **2014**, *16*, 4919−4926.
(4) Santaclara, J. G.; Kapteijn, F.; Gascon, J.; van der Veen, M. A. Understanding metal-organic frameworks for photocatalytic solar fuel production. *CrystEngComm* **2017**, *19*, 4118−4125.
(5) Cavka, J. H.; Jakobsen, S.; Olsbye, U.; Guillou, N.; Lamberti, C.; Bordiga, S.; Lillerud, K. P. A New Zirconium Inorganic Building Brick Forming Metal Organic Frameworks with Exceptional Stability. *J. Am. Chem. Soc.* **2008**, *130*, 13850−13851.
(6) Gomes Silva, C.; Luz, I.; Llabrés i Xamena, F. X.; Corma, A.; García, H. Water Stable Zr−Benzenedicarboxylate Metal−Organic Frameworks as Photocatalysts for Hydrogen Generation. *Chem. - Eur. J.* **2010**, *16*, 11133−11138.
(7) Hendrickx, K.; Vanpoucke, D. E. P.; Leus, K.; Lejaeghere, K.; Van Yperen-De Deyne, A.; Van Speybroeck, V.; Van Der Voort, P.; Hemelsoet, K. Understanding Intrinsic Light Absorption Properties of UiO-66 Frameworks: A Combined Theoretical and Experimental Study. *Inorg. Chem.* **2015**, *54*, 10701−10710.
(8) Kim, M.; Cahill, J. F.; Fei, H.; Prather, K. A.; Cohen, S. M. Postsynthetic Ligand and Cation Exchange in Robust Metal−Organic Frameworks. *J. Am. Chem. Soc.* **2012**, *134*, 18082−18088.
(9) Marshall, R. J.; Forgan, R. S. Postsynthetic Modification of Zirconium Metal-Organic Frameworks. *Eur. J. Inorg. Chem.* **2016**, *27*, 4310−4331.
(10) Chavan, S. M.; Shearer, G. C.; Svelle, S.; Olsbye, U.; Bonino, F.; Ethiraj, J.; Lillerud, K. P.; Bordiga, S. Synthesis and Characterization of Amine-Functionalized Mixed-Ligand Metal−Organic Frameworks of UiO-66 Topology. *Inorg. Chem.* **2014**, *53*, 9509−9515.
(11) Hendon, C. H.; Tiana, D.; Fontecave, M.; Sanchez, C.; D'Arras, L.; Sassoye, C.; Rozes, L.; Mellot-Draznieks, C.; Walsh, A. Engineering the Optical Response of the Titanium-MIL-125 Metal-Organic Framework through Ligand Functionalization. *J. Am. Chem. Soc.* **2013**, *135*, 10942−10945.
(12) Nasalevich, M. A.; Goesten, M. G.; Savenije, T. J.; Kapteijn, F.; Gascon, J. Enhancing optical absorption of metal-organic frameworks for improved visible light photocatalysis. *Chem. Commun.* **2013**, *49*, 10575−10577.
(13) Lee, Y.; Kim, S.; Kang, J. K.; Cohen, S. M. Photocatalytic CO_2 reduction by a mixed metal (Zr/Ti), mixed ligand metal-organic framework under visible light irradiation. *Chem. Commun.* **2015**, *51*, 5735−5738.
(14) Yasin, A. S.; Li, J.; Wu, N.; Musho, T. Study of the inorganic substitution in a functionalized UiO-66 metal-organic framework. *Phys. Chem. Chem. Phys.* **2016**, *18*, 12748−12754.
(15) Sun, D.; Liu, W.; Qiu, M.; Zhang, Y.; Li, Z. Introduction of a mediator for enhancing photocatalytic performance via post-synthetic metal exchange in metal-organic frameworks (MOFs). *Chem. Commun.* **2015**, *51*, 2056−2059.
(16) Wang, A.; Zhou, Y.; Wang, Z.; Chen, M.; Sun, L.; Liu, X. Titanium incorporated with UiO-66(Zr)-type Metal-Organic Framework (MOF) for photocatalytic application. *RSC Adv.* **2016**, *6*, 3671−3679.
(17) Brozek, C. K.; Dinca, M. Cation exchange at the secondary building units of metal-organic frameworks. *Chem. Soc. Rev.* **2014**, *43*, 5456−5467.
(18) Lalonde, M.; Bury, W.; Karagiaridi, O.; Brown, Z.; Hupp, J. T.; Farha, O. K. Transmetalation: routes to metal exchange within metal-organic frameworks. *J. Mater. Chem. A* **2013**, *1*, 5453−5468.
(19) Smith, S. J. D.; Ladewig, B. P.; Hill, A. J.; Lau, C. H.; Hill, M. R. Post-synthetic Ti Exchanged UiO-66 Metal-Organic Frameworks that Deliver Exceptional Gas Permeability in Mixed Matrix Membranes. *Sci. Rep.* **2015**, *5*, 7823.
(20) Hon Lau, C.; Babarao, R.; Hill, M. R. A route to drastic increase of CO_2 uptake in Zr metal organic framework UiO-66. *Chem. Commun.* **2013**, *49*, 3634−3636.
(21) Nguyen, H. G. T.; Mao, L.; Peters, A. W.; Audu, C. O.; Brown, Z. J.; Farha, O. K.; Hupp, J. T.; Nguyen, S. T. Comparative study of titanium-functionalized UiO-66: support effect on the oxidation of cyclohexene using hydrogen peroxide. *Catal. Sci. Technol.* **2015**, *5*, 4444−4451.
(22) Destefano, M. R.; Islamoglu, T.; Garibay, S. J.; Hupp, J. T.; Farha, O. K. Room-Temperature Synthesis of UiO-66 and Thermal Modulation of Densities of Defect Sites. *Chem. Mater.* **2017**, *29*, 1357−1361.
(23) Cliffe, M. J.; Wan, W.; Zou, X.; Chater, P. A.; Kleppe, A. K.; Tucker, M. G.; Wilhelm, H.; Funnell, N. P.; Coudert, F. X.; Goodwin, A. L. Correlated defect nanoregions in a metal-organic framework. *Nat. Commun.* **2014**, *5*, 4176.
(24) Shearer, G. C.; Chavan, S.; Ethiraj, J.; Vitillo, J. G.; Svelle, S.; Olsbye, U.; Lamberti, C.; Bordiga, S.; Lillerud, K. P. Tuned to Perfection: Ironing Out the Defects in Metal−Organic Framework UiO-66. *Chem. Mater.* **2014**, *26*, 4068−4071.
(25) Fang, Z.; Bueken, B.; De Vos, D. E.; Fischer, R. A. Defect-Engineered Metal−Organic Frameworks. *Angew. Chem., Int. Ed.* **2015**, *54*, 7234−7254.
(26) Ling, S.; Slater, B. Dynamic acidity in defective UiO-66. *Chem. Sci.* **2016**, *7*, 4706−4712.
(27) Trickett, C. A.; Gagnon, K. J.; Lee, S.; Gándara, F.; Bürgi, H.-B.; Yaghi, O. M. Definitive Molecular Level Characterization of Defects in UiO-66 Crystals. *Angew. Chem., Int. Ed.* **2015**, *54*, 11162−11167.
(28) Shearer, G. C.; Vitillo, J. G.; Bordiga, S.; Svelle, S.; Olsbye, U.; Lillerud, K. P. Functionalizing the Defects: Postsynthetic Ligand Exchange in the Metal Organic Framework UiO-66. *Chem. Mater.* **2016**, *28*, 7190−7193.
(29) Bristow, J. K.; Svane, K. L.; Tiana, D.; Skelton, J. M.; Gale, J. D.; Walsh, A. Free Energy of Ligand Removal in the Metal−Organic Framework UiO-66. *J. Phys. Chem. C* **2016**, *120* (17), 9276−9281.
(30) Katz, M. J.; Brown, Z. J.; Colon, Y. J.; Siu, P. W.; Scheidt, K. A.; Snurr, R. Q.; Hupp, J. T.; Farha, O. K. A facile synthesis of UiO-66, UiO-67 and their derivatives. *Chem. Commun.* **2013**, *49*, 9449−9451.
(31) Yang, D.; Odoh, S. O.; Wang, T. C.; Farha, O. K.; Hupp, J. T.; Cramer, C. J.; Gagliardi, L.; Gates, B. C. Metal−Organic Framework Nodes as Nearly Ideal Supports for Molecular Catalysts: NU-1000- and UiO-66-Supported Iridium Complexes. *J. Am. Chem. Soc.* **2015**, *137*, 7391−7396.
(32) Furukawa, H.; Gándara, F.; Zhang, Y.-B.; Jiang, J.; Queen, W. L.; Hudson, M. R.; Yaghi, O. M. Water Adsorption in Porous Metal−Organic Frameworks and Related Materials. *J. Am. Chem. Soc.* **2014**, *136*, 4369−4381.
(33) Kapilashrami, M.; Zhang, Y.; Liu, Y.-S.; Hagfeldt, A.; Guo, J. Probing the Optical Property and Electronic Structure of TiO2 Nanomaterials for Renewable Energy Applications. *Chem. Rev.* **2014**, *114*, 9662−9707.
(34) Scanlon, D. O.; Dunnill, C. W.; Buckeridge, J.; Shevlin, S. A.; Logsdail, A. J.; Woodley, S. M.; Catlow, C. R. A.; Powell, M. J.;

DOI: 10.1021/acs.chemmater.7b03320
Chem. Mater. 2017, 29, 8963−8967

Palgrave, R. G.; Parkin, I. P.; Watson, G. W.; Keal, T. W.; Sherwood, P.; Walsh, A.; Sokol, A. A. Band alignment of rutile and anatase TiO_2. *Nat. Mater.* **2013**, *12*, 798.
(35) Walsh, A.; Butler, K. T.; Hendon, C. H. Chemical principles for electroactive metal−organic frameworks. *MRS Bull.* **2016**, *41*, 870−876.
(36) Nasalevich, M. A.; Hendon, C. H.; Santaclara, J. G.; Svane, K.; van der Linden, B.; Veber, S. L.; Fedin, M. V.; Houtepen, A. J.; van der Veen, M. A.; Kapteijn, F.; Walsh, A.; Gascon, J. Electronic origins of photocatalytic activity in d0 metal organic frameworks. *Sci. Rep.* **2016**, *6*, 23676.
(37) Schrauben, J. N.; Hayoun, R.; Valdez, C. N.; Braten, M.; Fridley, L.; Mayer, J. M. Titanium and Zinc Oxide Nanoparticles Are Proton-Coupled Electron Transfer Agents. *Science* **2012**, *336*, 1298−1301.
(38) Dan-Hardi, M.; Serre, C.; Frot, T.; Rozes, L.; Maurin, G.; Sanchez, C.; Férey, G. A New Photoactive Crystalline Highly Porous Titanium(IV) Dicarboxylate. *J. Am. Chem. Soc.* **2009**, *131*, 10857−10859.
(39) Kuznetsov, A. I.; Kameneva, O.; Bityurin, N.; Rozes, L.; Sanchez, C.; Kanaev, A. Laser-induced photopatterning of organic-inorganic TiO_2-based hybrid materials with tunable interfacial electron transfer. *Phys. Chem. Chem. Phys.* **2009**, *11*, 1248−1257.
(40) Ramesha, G. K.; Brennecke, J. F.; Kamat, P. V. Origin of Catalytic Effect in the Reduction of CO_2 at Nanostructured TiO_2 Films. *ACS Catal.* **2014**, *4*, 3249−3254.
(41) Trousselet, F.; Archereau, A.; Boutin, A.; Coudert, F.-X. Heterometallic Metal−Organic Frameworks of MOF-5 and UiO-66 Families: Insight from Computational Chemistry. *J. Phys. Chem. C* **2016**, *120* (43), 24885−24894.

■ NOTE ADDED AFTER ASAP PUBLICATION

During revision of this paper we became aware of a relevant publication[41] detailing the thermodynamics of Ti incorporation in UiO-type clusters. In that paper, Ti inclusion into the SBU was shown to be largely endothermic further supporting the conclusions detailed in this paper. This article was published ASAP on October 19, 2017, without ref 41. The version of the paper that includes ref 41 was published ASAP on October 31, 2017.

DOI: 10.1021/acs.chemmater.7b03320
Chem. Mater. 2017, 29, 8963−8967